CrystEngComm

PAPER

View Article Online
View Journal | View Issue

Cite this: *CrystEngComm*, 2015, **17**, 81

Structural control: can [2 × 2] silver grids be formed from 4,5-disubstituted 3,6-di(2-pyridyl) pyridazines?†

Samantha E. Bodman, Anthony C. Crowther, Paul B. Geraghty and Christopher M. Fitchett*

Received 10th September 2014,
Accepted 1st November 2014

DOI: 10.1039/c4ce01851f

www.rsc.org/crystengcomm

The reaction of ligands based on 3,6-di(2-pyridyl)pyridazine with symmetrical carbocyclic rings fused to the pyridazine ring; 7,10-di(2-pyridyl)-8,9-diazafluoranthene (**L**$_1$), 1,4-di(2-pyridyl)-6,7,8,9-tetrahydro-5*H*-cyclo-hepta[*d*]pyridazine (**L**$_2$), 1,4-di(2-pyridyl)-5,6,7,8-tetrahydro-phthalazine (**L**$_3$), 1,4-di(2-pyridyl)-6,7-dihydro-5*H*-cyclo-penta[*d*]pyridazine (**L**$_4$) with silver salts gave a series of complexes (**1**–**7**). Characterisation of these using single crystal X-ray structure determination clearly showed that the steric bulk of the carbocycle affects the degree to which pyridine groups remain co-planar with pyridizine, and hence their ability to chelate. The more hindered ligands **L**$_1$–**L**$_3$ form a mixture of bischelating and tetrabridging, while the least hindered (**L**$_4$) was able to chelate exclusively. In the case of **L**$_4$, the nature of the anion and solvent were also able to affect the outcome of the reaction, with tetrafluoroborate giving the first example of a 4,5-substituted 3,6-di(2-pyridyl)pyridazine ring forming a [2 × 2]-grid.

Introduction

Metallosupramolecular chemistry utilises the coordination bond between metal atoms and organic ligands to self-assemble discrete and polymeric architectures. Such processes are greatly affected by the choice of ligand coordinating geometry[1] and preferred metal atom stereochemistry,[2] as well as type of anion and solvent.[3] The potential combinations give varied species including polygons, capsules, polymeric sheets and networks.[4] Supramolecular [*n x m*]-grids[5] are popular targets due to the typical close proximity of the metal atoms, which often allow electronic or magnetic communication between appropriate centres.[6] The principal requirement for grid formation is that the ligands used must provide parallel coordination to adjacent metal atoms, with early attention focussed on the [2 × 2]-grids formed from the combination of 3,6-di(2-pyridyl)pyridazine and tetrahedral metal atoms such as silver and copper(I), as shown in Scheme 1(a).[7] Substituted 3,3'-bipyridizines have also proven a popular platform for the self-assembly of larger [*n x m*]-grids, and, in combination with labile metal atoms, they often display structural isomerism, with the dynamic equilibrium between grids and helicates in solution demonstrated by Lehn with silver using pyridazine oligomers capped with 2-pyridyl groups.[8] The formation of face-to-face dimers and grids has also been observed with ligands containing a bridging pyridazine and other pendant donor group.[9] [*n x m*]-Grids can also be formed using metal atoms with octahedral geometry combined with tridentate ligands (Scheme 1(b)).[10]

We are interested in using [2 × 2]-grids based on 3,6-di(2-pyridyl)pyridazine as a structural motif for the construction of functional molecules by including substitution to the pyridazine ring.[11] The metallosupramolecular chemistry of 4-substituted or unsymmetrically 4,5-disubstituted

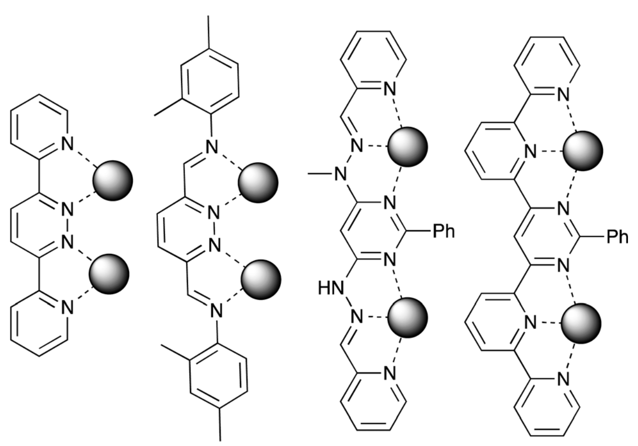

Scheme 1 Ligand systems previously used in the formation of grids using (a) bidentate ligands with tetrahedral metals such as Cu(I) and Ag, or (b) tridentate ligands with octahedral metals such as Co(II) and Zn, emphasising their parallel coordination of metal atoms.

Department of Chemistry, University of Canterbury, Christchurch 8140, New Zealand. E-mail: chris.fitchett@canterbury.ac.nz

† CCDC 1023446–1023452. For crystallographic data in CIF or other electronic format see DOI: 10.1039/c4ce01851f

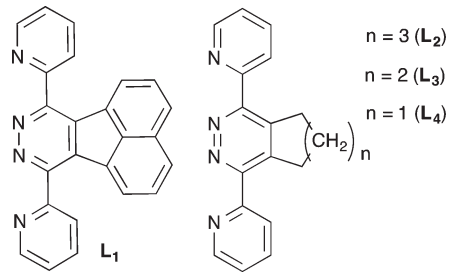

Scheme 2 Symmetrically substituted 3,6-di(2-pyridyl)pyridazine ligands used in this study.

3,6-di(2-pyridyl)pyridazines has been investigated by several groups, using a variety of metals including copper,[12] cadmium,[13] nickel,[14] ruthenium and iron,[15] with the observation that less symmetric substitution patterns lead to unsymmetrical coordination sites with differential binding and coordinated metal stereochemistry. In contrast, silver, which has a higher tolerance for unusual coordination geometries,[16] allows the formation of different architectures,[17] including side-by-side parallel coordination in the form of M_2L_2 face-to-face dimers.[18] Recently, a family of symmetrical ligands based on a 7,10-di(pyridin-2-yl)-8,9-diazafluoranthene core has been shown to give a range of similar architectures,[19] although, we note that the sole structurally characterised examples of [2 × 2]-grid formed between silver and these systems remain those of the parent 3,6-di(2-pyridyl)pyridazine.[7a]

Herein we describe the use of ligands (L_1–L_4) that retain the symmetry of the coordination sites, with particular focus on the effect of the addition of steric bulk remote from the coordinating system (Scheme 2). The investigation will use silver as the labile metal component, as this metal is known to act as a tetrahedral component in the formation of [2 × 2]-grids.

Results and discussion

Synthesis and solution studies of 1–7

The reaction of L_1 and L_2 with silver salts ($AgBF_4$ for L_1 and $AgPF_6$ for L_2) gave crystals of **1** and **2** suitable for X-ray structural analysis after diffusion of di-isopropyl ether into the reaction mixtures. The reaction of L_3 with AgOTf afforded colourless crystals (**3**). The reaction of L_4 with various silver salts gave crystals suitable for X-ray crystallography after diffusion of pentane into the reaction mixture (ClO_4 (**4**), PF_6 (**5**) and BF_4 (**6**)). All of these complexes were characterised in solution by NMR spectroscopy, which indicated that the solution structure of all the complexes involved symmetrical coordination, with the observation of the resonances for only a single pyridine ring. Interestingly, on standing in CD_3CN, the solution of **6** afforded crystals suitable for X-ray structural analysis of **7**.

Structural analysis

The structure of **1** showed that it had crystallised in the triclinic space group $P\bar{1}$, with two ligands, two metals and a dichloromethane solvate in the asymmetric unit. This structure is shown in Fig. 1, and has, not unexpectedly, the same supramolecular architecture as observed for the silver hexafluoroantimonate complex of the related ligand 2,5-di-*tert*-butyl-7,10-di(pyridin-2-yl)-8,9-diazafluoranthene.[19] Each of the distinct silver atoms are four coordinate, and approximately tetrahedral. While one of the ligands has the required parallel coordination of two metal atoms (Ag···Ag distance 3.8973(2) Å), the other bridges four metals, two through the central pyridazine ring and one through each pyridine ring. This bridging mode for a 3,6-(2-dipyridyl)-pyridazine based ligand is unusual, with two other examples of unsymmetrically substituted ligands bridging three silver atoms being the other highly substituted examples.[17,18] The different bridging modes of each ligand are controlled by the angle between the pyridine rings and the central pyridazine, with angles for the symmetrically chelating ligand of 59.80(13)° and 57.37(13)°, and angles of 121.15(12)° and 122.15(12)° for the tetradentate ligand. This twisting leads to the chelating ligand having significant pyramidalisation[20] of the nitrogen atoms, an effect that has been observed previously for similar ligands.[8a,21] In this case the pyridine ring nitrogens are 38.1(2)° and 37.1(2)° away from an ideal trigonal planar coordination, while the pyridizine nitrogen atom coordination is slightly less distorted with angles of 23.6(2)° and 22.9(2)°. The aromatic backbone is also distorted, with the nitrogen atoms of the pyridazine ring 0.675(6) Å out of the plane of the acenaphthylene section. These effects act to minimise the steric clash of the hydrogen atoms of the acenapthylene and pyridine rings (H···H = 2.53(1) Å). The tetracoordinate ligand is planar, and the coordinating nitrogen atoms do not exhibit significant pyramidalisation. The ligand geometry also creates an offset between the ligands, with the fused rings now sitting above the nitrogens of the adjacent pyridizine. The aromatic rings of L_1 form face-to-face π–π stacks to adjacent M_4L_4 units, with interactions occurring between the chelating ligands (centroid–centroid distance) arranging the subunits into 1-D tapes. The distortion of the chelating ligand also creates a pocket that contains the

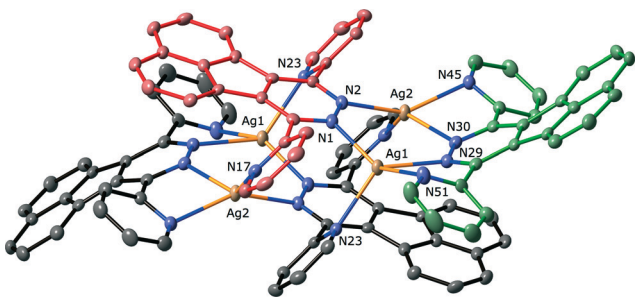

Fig. 1 Perspective view of **1** showing the chelating and bridging conformations of L_1 in green and red, respectively. Hydrogen atoms, counterions and solvate molecules have been removed for clarity, and thermal ellipsoids are shown at the 50% level. Selected bond lengths (Å): Ag1–N1 2.361(4), Ag1–N23^1 2.439(4), Ag1–N29 2.392(4), Ag1–N51 2.390(5), Ag2–N2 2.339(4), Ag2–N17^1 2.414(4), Ag2–N30 2.368(4), Ag2–N45 2.388(4). (Symmetry code: ^{1}1 − *x*, −*y*, 2 − *z*).

solvent molecules and counterions, although these have no strong interactions with any of the ligand clusters.

Complex **2** forms with a discrete subunit structure shown in Fig. 2, and has an asymmetric unit with one molecule of L_2, two equivalents of silver hexafluorophosphate and one non-coordinated DCM solvate, which was found on a centre of inversion. Here L_2 bridges four silver atoms in a manner similar to one of the L_1 molecules in the structure of **1**, with angles of 61.85(7)° and 65.85(8)° for the twisting of the pyridine rings *versus* the pyridazine ring, which is wide enough to prevent the ligand from chelating. The silver atoms are approximately tetrahedral, each coordinating to one pyridazine nitrogen, with the remaining sites taken up by acetonitrile solvate molecules. Interestingly one of these is hyperdentate[22] and bridges two of the silver atoms, with Ag–N bond distances slightly longer than for the monodentate acetonitrile molecules and a Ag–N–Ag angle of 102.45(9)°. The difference in the twisting of the ligand allows a closer approach of the silver atoms, with the Ag···Ag distance of 3.0182(2) Å for silver atoms across the discrete unit (compared with an Ag···Ag distance of 4.9531(4) Å for the equivalent interaction in **1**). As was observed above, the conformation of L_2 is controlled by the steric interaction between the hydrogens of the backbone (C–H···plane 2.238(2) and 2.242(2) Å). The conformation of the fused cycloheptane and coordinated acetonitrile molecules creates a pocket that holds one of the PF_6 anions, as shown in Fig. 2. The remaining dichloromethane solvate and counterion exist in the space between the subunits, with no significant interactions between them and the coordinated L_2 or acetonitrile molecules (F19···H32C 2.384(2) Å).

Complex **3** crystallises in the orthorhombic space group *Cmce* with two half molecules of L_3, one silver triflate and some disordered solvate (dichloromethane and acetonitrile) in the asymmetric unit. The M_4L_4 structure is similar to that formed in complex **1**, as shown in Fig. 3, containing two ligands with different conformations, one that chelates two silver atoms and another that bridges four silver atoms. Again this difference is evident in the degree of tilting of the pyridine rings *versus* the central pyridazine ring (chelating 45.8(1)° and tetracoordinate 111.3(1)°), and the distorted nature of the chelating ring leads to a significant pyramidalisation of the pyridine nitrogen atoms (32.5(1)°). The ligand distortion arises from the steric clash of the pyridine rings with a methylene of the alkyl ring (C–H···plane 2.343(2) Å and 2.256(2) Å), although this is complicated by disorder of the backbone of the bischelating ligand. The twisting of the tetracoordinate ligand also leads to the silver atoms across the subunit being further apart than complexes **2** (Ag···Ag distance 4.8020(1) Å). The ligands are offset and the pyridine rings of the tetracoordinate ligand molecule able to form a π–π stack across the M_4L_4 unit. The silver atom adopts an approximate tetrahedral geometry, and is coordinated by two pyridine rings and two pyridazine rings with distances ranging from 2.344(2) Å to 2.392(2) Å.

The complexes **4** and **5** both have the same discrete face-to-face M_2L_2 dimer structure, with that of **5** shown in Fig. 4. In each complex, an inversion centre relates the two halves of the macrocycles, with each independent ligand chelating two metal atoms. Clearly in this case the chelation of two metal atoms per ligand is not precluded by the steric clash between the pyridine rings and the methylene groups. The pyridine rings are twisted much less than any of the examples described above (37.5(1)° and 27.1(1)° for **4**, and 29.3(1)° and 31.8(1)° for **5**), with this twisting attributed to the steric clash between the $-CH_2-$ of the alkyl ring and the

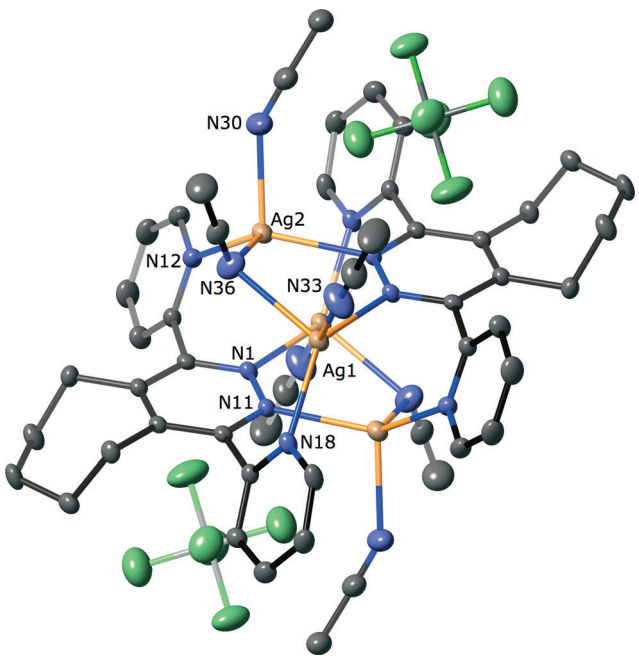

Fig. 2 Perspective view of **2**, showing the hyperdentate acetonitrile and anion pocket. Hydrogen atoms and solvate molecules have been removed for clarity, and thermal ellipsoids are shown at the 50% level. Selected bond lengths (Å): Ag1–Ag2 3.0182(3), Ag1 N1 2.3346(18), Ag1 $N18^1$ 2.296(2), Ag1 N33 2.268(3), Ag1 N36 2.534(2), Ag2 $N11^1$ 2.4181(18), Ag2 N12 2.319(2), Ag2 N30 2.310(2), Ag2 $N36^1$ 2.404(2). (Symmetry code: $^1 1 - x, 1 - y, -z$).

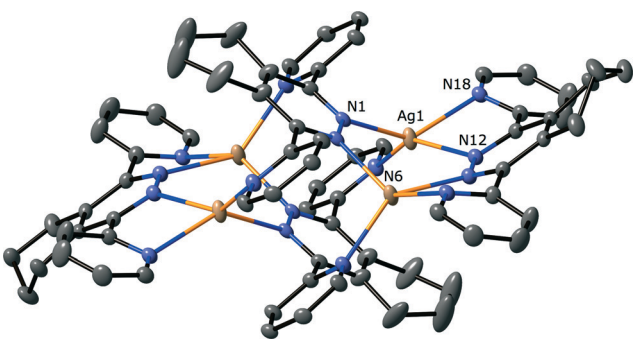

Fig. 3 Perspective view of **3** showing the chelating and bridging conformations of L_3. Hydrogen atoms, counterions and solvate molecules have been removed for clarity, and thermal ellipsoids are shown at the 50% level. Selected bond lengths (Å): Ag1–N1 2.344(2), Ag1–$N6^1$ 2.366(2), Ag1–N12 2.367(2), Ag1–N18 2.3918(19). (Symmetry code: $^1 1 - x, 1 - y, 1 - z$).

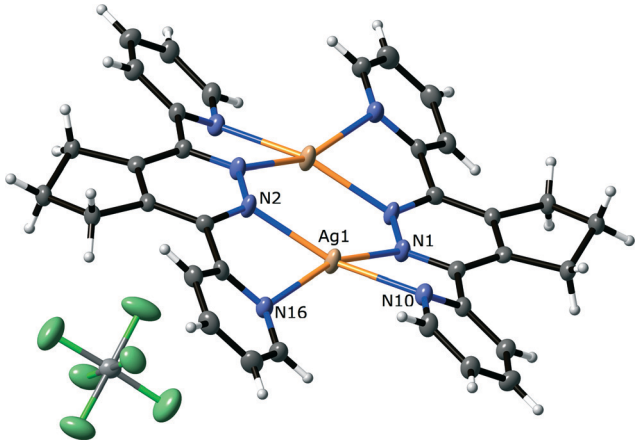

Fig. 4 Perspective view of **5**. Thermal ellipsoids are shown at the 50% level. Selected bond lengths (Å): Ag1–N1 2.300(3), Ag1–N2^{1} 2.286(3), Ag1–N10 2.355(3), Ag1–N16^{1} 2.362(3). (Symmetry code: $^{1}1-x, 1-y, 1-z$).

pyridine ring. The increased co-planarity of the rings leads to less pyramidalisation of the coordinated nitrogen atoms (26.2(2)° and 19.4(2)° for **4**, and 26.7(2)° and 27.9(2)° for **5**), while the silver atoms are tetracoordinate and have a distorted square planar geometry,[23] and are held 3.6056(2) Å and 3.5466(2) Å apart for **4** and **5**, respectively. The subunits are able to form π–π stacks with centroid-to-centroid distances of 3.638(2) Å for **4**, and 3.740(3) for **5**, although these only involve the pyridine rings. This is due to a combination of the conformation of the fused cyclopentene ring and the perchlorate or hexafluorophosphate counterions which occupy space above adjacent units. Complex **5** also contains a disordered dichloromethane solvate, although this forms only weak interactions with surrounding anions or the M_2L_2 dimer.

Complex **6** was found to have a [2 × 2]-grid like structure, as shown in Fig. 5. The complex crystallises in the monoclinic space group *P*2/*n* and consists of two independent half-grids and their associated anions, two dichloromethane solvates and one water molecule. Interestingly there is no acetonitrile present in the complex, perhaps indicating that the formation of **6** and **7** under different solvent conditions is due to preferential crystallisation of an equilibrium mixture. Unlike the structure of **5** observed above, the molecules of $\mathbf{L_4}$ each chelate two metal atoms. The nitrogen to silver bond distances range from 2.072(6) Å to 2.628(8) Å, although the longer of these is affected by positional disorder of the silver atoms of one grid (modelled as ≈ 1 : 1). Two of the silver atoms of each grid lie on a two-fold axis, with all silver atoms having approximate tetrahedral geometry. In a similar manner to the ligand conformations observed in **5**, the pyridine rings of $\mathbf{L_4}$ are twisted to a lesser degree than for the other ligands in this study (18.2(2)–28.6(2)°), and there is no significant pyramidalisation of the metal atoms.

The [2 × 2]-grids are both slightly tilted (Fig. 6), as defined by the interplanar angles between the pyridizine of 78.6(1)° and 70.5(1)° for the ordered and disordered grid, respectively,

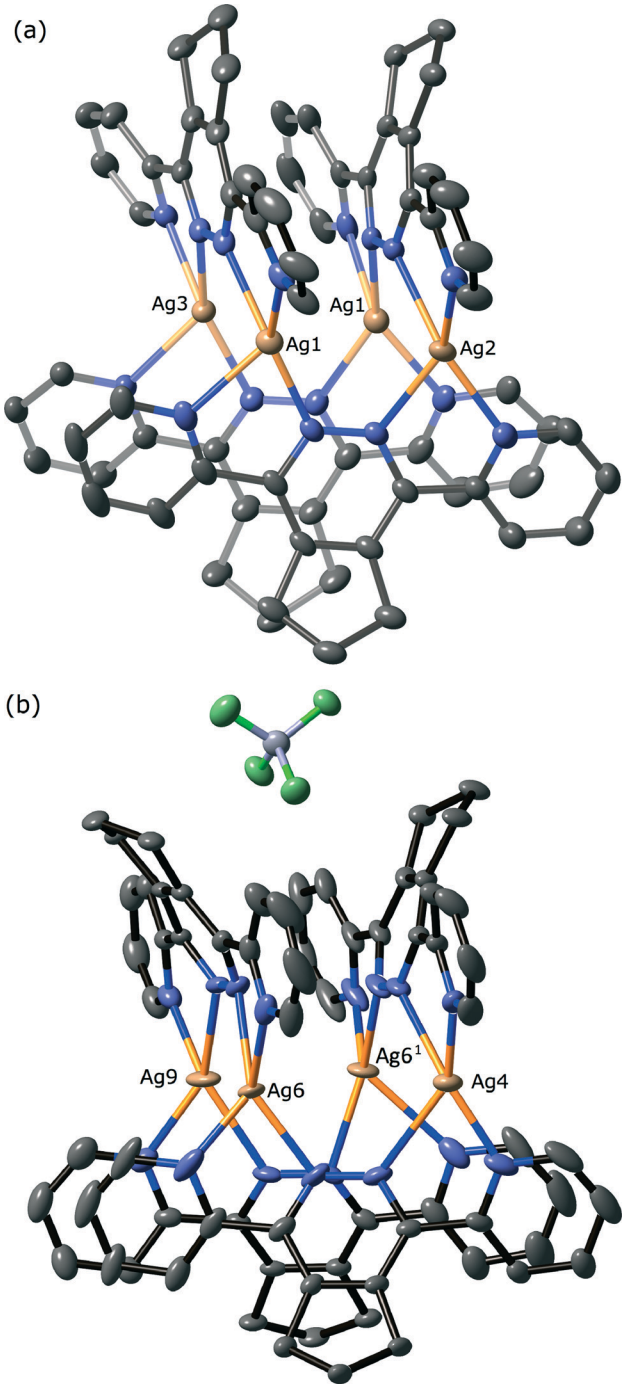

Fig. 5 Perspective views of the two independent [2 × 2]-grids of **6**, indicating the different orientations of the cyclopentane rings, showing (a) the closed grid, and (b) the open grid including the tetrafluoroborate anion occupying the space created by the clip. Hydrogen atoms and remaining anions have been removed for clarity, and thermal ellipsoids are shown at the 30% level.

ideal for a square grid is 90°. This tilting allows the aromatic rings of each grid to form offset face-to-face π–π across the stacks between adjacent pyridine rings having centroid-to-centroid distances ranging between 3.641(2)–3.900(2) Å. The tilting also causes the silver atoms to describe the corners of

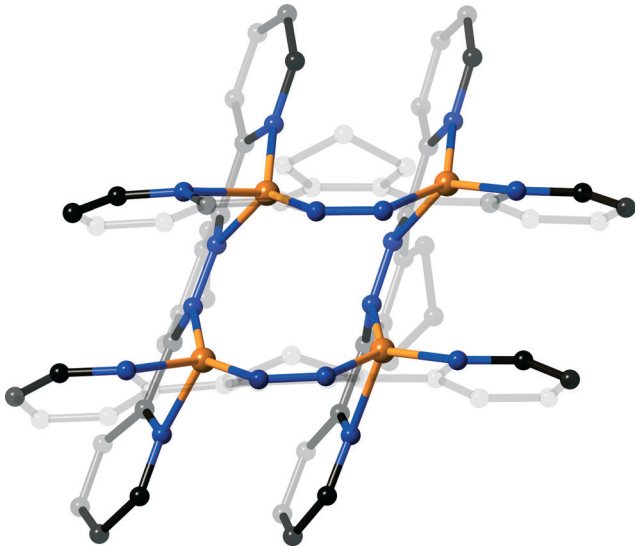

Fig. 6 View of one of the [2 × 2]-grids of **6** showing the tilting of the grids, and the distances between silver atoms. The molecules of L_4 have been faded to emphasise the geometry of the nitrogen atoms that surround each silver atom.

an almost rhombohedral parallelogram, with distances along the sides ranging from 3.420(1)–3.712(1) Å, whilst the distances across fall into either short (3.801(1)–3.923(1) Å) and long (5.616(1)–6.033(1) Å). The central pyridazine rings of each of the independent grids differ in their relative orientation, as affected by the fused cyclopentene ring. In the case of the 'closed' ordered grid (Fig. 5(a)), the cyclopentane rings are oriented towards one another, allowing the pyridazine rings to form a face-to-face π–π stack (centroid-to-centroid distance 3.785(4) Å), whilst in the 'open' less ordered grid these rings are tilted away from one-another (Fig. 7(b)) causing the pyridazine rings to lack the coplanarity required to form a face-to-face π–π stack (46.9(2)°). This open orientation

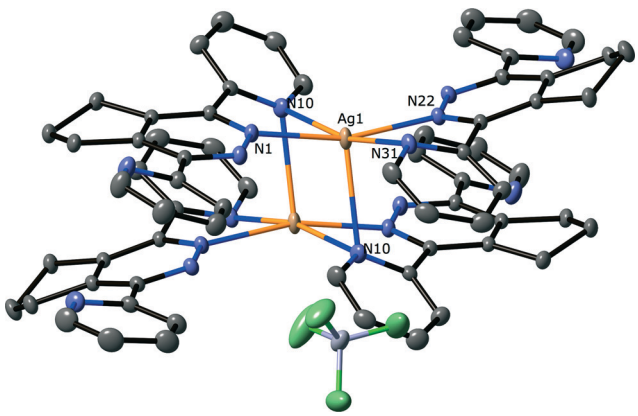

Fig. 7 Perspective view of **7**, showing the orientation of the pendant pyridine rings and the hyperdentate nitrogen atom (N10). Hydrogen atoms have been omitted for clarity and thermal elipsoids are shown at the 50% level. Selected bond lengths (Å): Ag1–N1 2.2793(8), Ag1–N10 2.4998(10), Ag1–N22 2.2842(8), Ag1–N31 2.4909(9), Ag1–N10^1 2.6627(10). (Symmetry code: ^{1} –*x*, 1 – *y*, –*z*).

allows this grid to form a clip around a tetrafluoroborate counterion, with the closest approach being between a $-CH_2-$ and the anion having an H···F distance of 2.500(4) Å, indicating a weak interaction. The other anions and solvate show no significant interactions with the grids.

The complex isolated from d_3-acetonitrile (**7**) consists of two ligands that chelate a single silver atom, as shown in Fig. 7, a structure that has previously been observed for 3,6-di(2-pyridyl)pyridazine and silver triflate.[12b] The ligands also have uncoordinated pyridine rings on opposite sides of the silver atom, which are oriented to remove the steric clash of the hydrogen atoms, a common conformation for biheterocycles.[24] The coordinated pyridine rings are twisted relative to the central pyridazine ring more than the uncoordinated rings (18.08(4)° and 23.09(4)° *vs.* 27.72(4)° and 38.10(4)°) to relieve the steric clash observed above. This twisting leads to pyramidalisation of the coordinated pyridine nitrogen atom, as observed above, with this nitrogen hyperdentate and bridging two silver atoms as shown in Fig. 7. This unusual geometry has been observed on a few occasions in terpyridine complexes of silver, where the twisting of the pyridine rings allows one ring to bridge two symmetrically equivalent metal atoms through a nitrogen atom.[25] The coordination bond lengths for the hyperdentate nitrogen, N10–Ag1 distances 2.500(1) Å and 2.663(1) Å, are approximately in the middle of the observed range. The silver atom has a slightly distorted square planar geometry, with the silver involved in weak metal–metal interaction (Ag···Ag distance 2.9925(2) Å), which pulls the silver slightly out of the N4 plane. Due to their close proximity, an adjacent pair of ligands form π–π interactions between the three heterocyclic rings, with centroid–centroid distances of 3.576(1), 3.784(1) and 3.780(1) Å.

The variability in the structures of **4**–**8**, all formed with L_4, illustrates the considerable effect of the reaction solvent and counterion. In **4**–**7** the ligands all have the parallel coordination required for the formation of [2 × 2]-grids, although only in the case of tetrafluoroborate was this realised. The difference between **7** and **8** is the lack of dichloromethane in the formation of the latter. Such observations are common in the supramolecular chemistry of silver, where the lability of silver–ligand bond allows subtle anion[26] and solvent[27] effects to play a greater role. The similarity of the ^{1}H-NMR data for these complexes indicates that the anion and solvent have a limited effect on their structures in solution. In each of these complexes the anions played only ancillary structural roles, remaining uncoordinated to the metal centre, and have only weak interactions with the ligands. We believe the differences in their solid-state structures are due to packing effects and these weak interactions.

Conclusions

The investigation of the reaction of a series of 3,6-di(2-pyridyl)pyridazine derivatives, with a variety of carbocyclic ring systems fused across the 4,5-pyridazine bond has lead to a range of complexes. The fused groups clearly affect the

Table 1 Crystal data and parameter for **1–8**

Compound	**1**	**2**	**3**	**4**
Empirical formula	$C_{50.75}H_{33.5}Ag_2B_2Cl_{5.5}F_8N_8$	$C_{26}H_{29}Ag_2Cl_2F_{12}N_7P_2$	$C_{79.5}H_{66}Ag_4Cl_2F_{12}N_{18}O_{12}S_4$	$C_{17}H_{14}AgClN_4O_4$
Formula weight	1339.69	1016.14	2324.12	481.64
Radiation source	Mo Kα	Mo Kα	Mo Kα	Mo Kα
Temperature (K)	105(1)	120.0(1)	105(1)	105(1)
Crystal system	Triclinic	Triclinic	Orthorhombic	Triclinic
Space group	$P\bar{1}$	$P\bar{1}$	*Cmce*	$P\bar{1}$
Unit cell dimensions: a (Å)	10.6406(5)	10.8963(2)	17.1919(4)	8.0993(4)
b (Å)	15.5529(8)	13.6018(4)	17.6525(5)	9.7117(4)
c (Å)	16.8867(12)	13.9028(4)	28.3109(8)	11.2515(5)
α (°)	66.629(3)	109.104(3)	90	87.315(3)
β (°)	87.281(4)	94.569(2)	90	86.505(3)
γ (°)	81.087(3)	109.486(2)	90	68.644(2)
Volume (Å^3)	2534.1(3)	1793.82(9)	8591.8(4)	822.43(7)
Z	2	2	4	2
Density (calculated) (Mg m^{-3})	1.756	1.881	1.797	1.945
Absorption coefficient (mm^{-1})	1.139	1.424	1.156	1.423
F(000)	1327.0	1000.0	4636.0	480.0
Crystal size (mm)	0.4 × 0.06 × 0.05	0.29 × 0.28 × 0.19	0.28 × 0.23 × 0.13	0.33 × 0.31 × 0.14
Theta range for data collection (°)	4.648 to 51.998°	5.48 to 59.994°	4.614 to 59.988°	5.406 to 58.288
Reflections collected	16 756	30 541	112 774	19 803
Independent reflections [$R_{(int)}$]	16 756 [0.0573]	10 454 [0.0241]	6462 [0.0587]	4385 [0.0487]
Observed reflections ($I > 2\sigma(I)$)	12 764	9310	5140	3550
Data/restraints/parameters	16 756/0/724	10 454/0/463	6462/12/342	4385/0/244
Goodness-of-fit on F^2	1.023	1.045	1.053	1.039
R_1 [$I > 2\sigma$ (I)]	0.0476	0.0325	0.0343	0.0358
wR_2 (all data)	0.1140	0.0902	0.0996	0.0923

	5	**6**	**7**
Empirical formula	$C_{17.5}H_{14}AgClF_6N_4P$	$C_{70}H_{62}Ag_4B_4Cl_4F_{16}N_{16}O$	$C_{34}H_{28}AgBF_4N_8$
Formula weight	568.62	2063.87	743.32
Radiation source	Mo Kα	Cu Kα	Mo Kα
Temperature (K)	105(1)	120.0(1)	120.0(1)
Crystal system	Monoclinic	Monoclinic	Triclinic
Space group	$P2_1/n$	$P2/n$	$P\bar{1}$
Unit cell dimensions: a (Å)	8.5680(3)	23.76695(15)	7.72940(14)
b (Å)	26.1905(8)	13.12396(9)	13.2469(2)
c (Å)	8.6188(2)	25.09710(17)	15.3754(3)
α (°)	90	90	78.2170(15)
β (°)	95.015(2)	102.5639(7)	81.8669(14)
γ (°)	90	90	77.2006(15)
Volume (Å^3)	1926.66(10)	7640.74(9)	1495.17(5)
Z	4	4	2
Density (calculated) (Mg m^{-3})	1.960	1.794	1.651
Absorption coefficient (mm^{-1})	1.338	10.224	0.741
F(000)	1120.0	4013.0	752.0
Crystal size (mm)	0.23 × 0.17 × 0.08	0.24 × 0.23 × 0.12	0.28 × 0.12 × 0.05
Theta range for data collection (°)	4.992 to 54.988°	5.788 to 151.932°	5.432 to 75.386°
Reflections collected	37 629	81 531	65 436
Independent reflections [$R_{(int)}$]	4422[0.0644]	15 848[0.0271]	15 329[0.0336]
Observed reflections ($I > 2\sigma(I)$)	3549	13 529	13 643
Data/restraints/parameters	4422/0/286	15 848/0/1081	15 329/0/433
Goodness-of-fit on F^2	1.078	1.042	1.073
R_1 [$I > 2\sigma(I)$]	0.0381	0.0586	0.0280
wR_2 (all data)	0.0977	0.1671	0.0742

degree to which the pyridine rings were able to remain co-planar with the pyridazine, controlling whether the ligands are able to simultaneously chelate two or bridge four silver atoms as monodentate donors. Here, $\mathbf{L_2}$ only formed as a tetrabridging unit, indicating that it has the largest fused group. In contrast $\mathbf{L_1}$ and $\mathbf{L_3}$ were able to sustain both bischelating and tetrabridging in the same complex. In the case of $\mathbf{L_4}$, the least hindered fused group allows the ligand molecule to chelate in all the complexes isolated. The effect of the anion in these structures was considerable, with three different structural motifs isolated. This includes, to the best of our knowledge, the first example of a 3,6-di(2-pyridyl)-pyridazine substituted in the pyridazine ring forming a [2 × 2]-grid. We are currently investigating the extent to which this substitution can be extended to determine the utility of these complexes as supramolecular building blocks.

Experimental

All reagents and starting materials were reagent grade, obtained from commercial sources and used as received, unless otherwise stated. NMR spectra were recorded at 23 °C on Varian INOVA 400 or Varian Unity INOVA 500 spectrometers, operating for ^{1}H, at 400 MHz and 500 MHz, respectively and for ^{13}C, at 100 MHz and 125 MHz, respectively. Commercially available deuterated solvents ($CDCl_3$, CD_3CN and DMSO) were used with tetramethylsilane (TMS) as an internal reference. Elemental analysis was carried out by the Campbell Microanalytical Laboratory, located at The University of Otago. Electrospray ionisation mass spectra (HR-ESMS) were recorded on a Bruker MaXis 4G spectrometer operated in high-resolution positive ion electrospray mode. Infrared spectra were recorded on a Bruker ALPHA FT-IR spectrometer with diamond ATR configuration, DTGS 4000–430 cm^{-1}. All the ligands for this study were synthesized using the appropriate literature method.[28] *Caution! Perchlorate salts are potentially explosive and special care should be taken while handling those compounds*.

AgOTf with 7,10-di(pyridin-2-yl)-8,9-difluoranthene (1)

Two solutions, one of $\mathbf{L_1}$ (12.0 mg, 0.0335 mmol) in hot dichloromethane (2 ml) and another of silver tetrafluoroborate (12.1 mg, 0.0623 mmol) in hot dichloromethane and acetonitrile (9 : 1) were combined. Crystals were obtained after vapour diffusion of diisopropyl ether into the reaction mixture. Yield: 52.1%. Mp: >360 °C. ^{1}H-NMR (400 MHz, DMSO) δ 8.95 (d, J = 4.3 Hz, 2H, H_6), 8.30–8.18 (m, 8H, $H_{11,3,13,4}$), 7.80–7.73 (m, 4H, $H_{12,5}$). ^{13}C-NMR (100 MHz, DMSO) δ 155.57 (C_2), 149.83 (C_6), 138.39 (C_4), 131.77 (C_{11}), 129.38 (C_{13}), 129.00 (C_{12}), 125.60 (C_5), 125.22 (C_3). IR ν/cm^{-1}: 3389br/w, 3067br/w, 1592w, 1416w, 1221s, 1142m, 1025s, 771m, 634s. ESI-MS: 825.1495 $[Ag(\mathbf{L_1})_2]^+$, 645.0883 $[Ag_2(\mathbf{L_1})_3]^{2+}$, 465.0264 $[Ag(\mathbf{L_1})]^+$/$[Ag_2(\mathbf{L_1})_2]^{2+}$, 359.1289 $[(\mathbf{L_1})H]^+$. UV-Visible (DMSO) λ_{max} (ε) 368 nm (11 912), 326 nm (11 610), 271 nm (25 892), 256 nm (25 103). Analysis: calc. for $C_{24}H_{14}N_4AgBF_4$: C, 52.12; H, 2.55; 10.13. Found: C, 52.55; H, 2.66; N, 10.15.

$AgPF_6$ with 1,4-di(pyridin-2-yl)-6,7,8,9-tetrahydro-5*H*-cyclohepta[*d*]pyridazine (2)

A reaction mixture of silver hexafluorophosphate (25.8 mg, 0.102 mmol) in hot dichloromethane and acetonitrile (9 : 1, 1 ml) and $\mathbf{L_2}$ (11.2 mg, 0.037 mmol) in hot dichloromethane (1 ml) gave crystals after vapour diffusion of pentane into the reaction mixture. Yield: 58.7%. Mp: 220 °C. ^{1}H-NMR (500 MHz, CD_3CN) δ 8.57 (d, J = 4.6 Hz, 1H, H_6), 8.01 (t, J = 7.7 Hz, 1H, H_4), 7.63 (d, J = 7.8 Hz, 1H, H_3), 7.54 (dd, J = 6.8 Hz, 5.6Hz, 1H, H_5), 2.87 (t, J = 5.1 Hz, 2H, H_{10}), 1.95–1.90 (m, 2H, H_{12}), 1.71–1.67 (m, 2H, H_{11}). ^{13}C-NMR (125 MHz, CD_3CN) δ 158.28 (C_8), 153.35 (C_2), 150.57 (C_6), 144.86 (C_9), 137.87 (C_4), 125.73 (C_3), 124.92 (C_5), 31.07 (C_{12}), 29.94 (C_{10}), 25.42 (C_{11}). IR ν/cm^{-1}: 2943br/w, 2267br/w, 1596w, 1007br/m, 825s, 555m. UV-Vis: (CH_3CN) λ_{max} (ε) 269 nm (18 979), 219 nm (30 875). ESI-MS: 965.0798 $[Ag_2(\mathbf{L_2})_2](PF_6)$, 561.1349 $[Ag_2(\mathbf{L_2})_3]^{2+}$, 409.0578 $[Ag(\mathbf{L_2})]^+$/$[Ag_2(\mathbf{L_2})_2]^{2+}$, 303.1604 $[(\mathbf{L_2})H]^+$. Analysis: calc. for $C_{19}H_{18}N_4(AgPF_6)_2{\cdot}(CH_3CN)_2{\cdot}CH_2Cl_2$: C, 29.56; H, 2.69; N, 8.62. Found C, 29.44; H, 2.50; N, 8.39.

AgOTf with 1,4-di(pyridin-2-yl)-5,6,7,8-tetrahydrophthalazine (3)

A solution of silver triflate (9.8 mg, 0.038 mmol) in warm dichloromethane and acetonitrile (9 : 1, 1 ml) was added to a warm solution of $\mathbf{L_3}$ (10.0 mg, 0.035 mmol) in dichloromethane (1 ml), giving a yellow solution. Vapour diffusion of pentane initially gave colourless crystals. Compound 3: Yield: 40.1% Mp: 222 °C. ^{1}H-NMR (500 MHz, CD_3CN) δ 8.56 (d, J = 4.9 Hz, 1H, H_6), 8.01 (t, J = 7.7 Hz, 1H, H_4), 7.77 (d, J = 7.8 Hz, 1H, H_3), 7.52 (m, 1H, H_5), 2.79 (s, 1H, H_{10}), 1.76 (s, 1H, H_{11}). ^{13}C-NMR (125 MHz, CD_3CN) δ 158.52 (C_8), 153.11 (C_2), 150.35 (C_6), 139.56 (C_9), 137.74 (C_4), 125.38 (C_3), 124.97 (C_5), 26.89 (C_{10}), 20.90 (C_{11}). IR ν/cm^{-1}: 2950br/w, 1595w, 1244s, 1149s, 1025s, 791w, 633s, 514w. UV-Vis: (CH_3CN) λ_{max} (ε) 271 nm (27 070). ESMS: 941.0365 $[Ag_2(\mathbf{L_3})_2](CF_3SO_3)$, 540.1112 $[Ag_2(\mathbf{L_3})_3]^{2+}$, 395.0421 $[Ag_2(\mathbf{L_3})_2]^{2+}$, 289.1447 $[(\mathbf{L_3})H]^+$. Analysis: calc. for $C_{18}H_{16}N_4{\cdot}AgCF_3SO_3{\cdot}1/4CH_2Cl_2$: C, 40.81; H, 2.94; N, 9.89. Found: C, 40.59; H, 3.01; N, 9.69.

$AgClO_4$ with 1,4-di(pyridin-2-yl)-6,7-dihydro-5*H*-cyclopenta[*d*]pyridazine (4)

Reaction of $\mathbf{L_4}$ (13.6 mg, 0.050 mmol) in hot dichloromethane (1 ml) and silver perchlorate (11.7 mg, 0.056 mmol) in hot dichloromethane and acetonitrile (9 : 1) gave a colourless solution. Large crystals were obtained after vapour diffusion of pentane into the reaction mixture. Yield: 63.0%. Mp: 245 °C. ^{1}H-NMR (500 MHz, CD_3CN) δ 8.69 (s, 1H, H_6), 8.09–8.06 (m, 2H, $H_{3,4}$), 7.62 (s, 1H, H_5), 3.34 (t, J = 7.1 Hz, 2H, H_{10}), 2.19–2.18 (m, 2H, H_{11}). ^{13}C-NMR (125 MHz, CD_3CN) δ 154.61 (C_2), 152.57 (C_8), 150.36 (C_6), 147.21 (C_9), 138.03 (C_4), 125.32 (C_5), 124.55 (C_3), 33.33 (C_{10}), 24.48 (C_{11}). IR ν/cm^{-1}: 2968br/w, 1593w, 1386w, 1068br/s, 788m, 618s. UV-Vis: (CH_3CN) λ_{max} (ε) 288 nm (28 263). ESMS: 863.0007 $[Ag_2(\mathbf{L_4})_2](ClO4)$, 655.1483 $[Ag(\mathbf{L_4})_2]^+$, 381.0206 $[Ag(\mathbf{L_4})]$+/$[Ag_2(\mathbf{L_4})_2]^{2+}$, 275.1287 $[(\mathbf{L_4})H]^+$. Analysis: calc. for $C_{17}H_{14}N_4{\cdot}AgClO_4{\cdot}H_2O$: C, 40.86; H, 3.23; N, 11.21. Found: C, 40.61; H, 3.50; N, 11.06.

$AgPF_6$ with 1,4-di(pyridin-2-yl)-6,7-dihydro-5*H*-cyclopenta[*d*]pyridazine (5)

A solution of silver hexafluorophosphate (7.6 mg, 0.030 mmol) in warm dichloromethane and acetonitrile (9 : 1, 1 ml) was added to a hot solution of $\mathbf{L_4}$ (7.3 mg, 0.028 mmol) in dichloromethane (1 ml), forming a pale yellow solution. Crystals were obtained after vapour diffusion of pentane into the reaction mixture. Yield: 53.6%. Mp: 227 °C. ^{1}H-NMR (500 MHz, CD_3CN) δ 8.70 (s, 1H, H_6), 8.10–8.05 (m, 2H, $H_{3,4}$), 7.62 (s, 1H, H_5), 3.34 (t, J = 7.5 Hz, 2H, H_{10}), 2.17–2.16 (m, 2H, H_{11}). ^{13}C-NMR (125 MHz, CD_3CN) δ 152.47 (C_2), 150.60 (C_6), 147.54 (C_9), 138.26 (C_4), 125.61 (C_5), 124.85 (C_3), 33.42 (C_{10}), 24.61 (C_{11}). IR ν/cm^{-1}: 2967br/w, 1588w, 1387w, 1133w, 827s, 554s. UV-Vis: (CH_3CN) λ_{max} (ε) 288 nm (14 003).

ESI-MS: 909.0179 $[Ag_2(L_4)_2](PF_6)$, 655.1493 $[Ag(L_4)_2]^+$, 381.0264 $[Ag(L_4)]^+/[Ag_2(L_4)_2]^{2+}$, 275.1288 $[(L_4)H]^+$. Analysis: calc. for $C_{17}H_{14}N_4{\cdot}AgPF_6$: C, 38.73; H, 2.68; N, 10.63. Found: C, 39.00; H, 2.66; N, 10.62.

$AgBF_4$ with 1,4-di(pyridin-2-yl)-6,7-dihydro-5*H*-cyclopenta[*d*]pyridazine (6)

Silver tetrafluoroborate (10.1 mg, 0.052 mmol) and L_4 (13.6 mg, 0.050 mmol) were dissolved separately in dichloromethane and acetonitrile (9 : 1, 3 ml) and dichloromethane (3 ml), respectively, heated, and then combined. Crystals were prepared by vapour diffusion of pentane into the mixture. Yield: 69.1%. Mp: 232 °C. ^{1}H-NMR (500 MHz, CD_3CN) δ 8.61 (d, J = 4.6 Hz, 1H, H_6), 8.03–8.02 (m, 2H, $H_{3,4}$), 7.56 (dd, J = 8.8 Hz, 4.3 Hz, 1H, H_5), 3.28 (t, J = 7.4 Hz, 2H, H_{10}), 2.15–2.11 (m, 2H, H_{11}). ^{13}C-NMR (125 MHz, CD_3CN) δ 154.44 (C_2), 151.97 (C_8), 150.56 (C_6), 147.39 (C_9), 138.18 (C_4), 125.54 (C_5), 124.77 (C_3), 33.28 (C_{10}), 24.52 (C_{11}). IR ν/cm^{-1}: 2970br/w, 1587w, 1444w, 1378w, ESI-MS: 851.0573 $[Ag_2(L_4)_2(BF_4)]^+$, 655.1492 $[Ag(L_4)_2]^+$, 519.0874 $[Ag_2(L_4)_3]^{2+}$, 381.0267 $[Ag(L_4)]^+/[Ag_2(L_4)_2]^{2+}$, 275.1291 $[(L_4)H]^+$. IR ν/cm^{-1}: 2957br/w, 1590w, 1467w, 1380w, 1032br/s, 789m, 743m, 519m. UV-Visible (CH_3CN) λ_{max} 288 nm. Analysis: calc. for $C_{17}H_{14}N_4{\cdot}AgBF_4{\cdot}1/2CH_2Cl_2$: C, 41.10; H, 2.96; N, 10.95. Found: C, 41.16; H, 3.06; N, 11.15.

$AgBF_4$ with 1,4-di(pyridin-2-yl)-6,7-dihydro-5*H*-cyclopenta[*d*]pyridazine (7)

Silver tetrafluoroborate (4.11 mg, 0.015 mmol) and L_4 (2.92 mg, 0.015 mmol) were dissolved in d_3-aceteonitile for NMR analysis. Overnight, yellow crystals formed in the NMR tube suitable for single crystal X-ray analysis. Yield: 54.2%. Mp: 242 °C IR ν/cm^{-1}: 2970br/w, 1587w, 1444w, 1378w, 1047br/s, 787m, 738m, 614w. UV-Vis: (CH_3CN) λ_{max} (ε) 288 nm (27 047). ESI-MS: 851.0569 $[Ag_2(L_4)_2](BF_4)$, 519.0875 $[Ag_2(L_4)_3]^{2+}$, 381.0267 $[Ag(L_4)]^+/[Ag_2(L_4)_2]^{2+}$, 275.1288 $[(L_4)H]^+$.

X-ray crystallography

X-ray crystallographic data collection and processing were carried out for complexes **1** and **3–5** on a Bruker ApexII diffractometer using Mo Kα (λ = 0.71073 Å) radiation and for complexes **2**, **6** and **7** on an Oxford-Agilent SuperNova instrument with focused microsource Cu Kα (λ = 1.51418 Å) radiation or Mo Kα (λ = 0.71073 Å), as indicated in Table 1, and an ATLAS CCD area detector. All data was collected at the temperature indicated. All structures were solved using direct methods with SHELXS[29] and refined on F^2 using all data by full matrix least-squares procedures with SHELXL-97 (ref. 30) within OLEX-2.3.[31] Non-hydrogen atoms were refined with anisotropic displacement parameters. Hydrogen atoms were placed in calculated positions or manually assigned from residual electron density where appropriate unless otherwise stated. The functions minimized were $\Sigma w(F^2_o - F^2_c)$, with w = $[\sigma 2(F^2_o) + aP2 + bP] - 1$, where $P = [\max(F_o)^2 + 2F^2c]/3$. The isotropic displacement parameters are 1.2 times the isotropic equivalent of their carrier atoms.

Acknowledgements

We would like to thank the University of Canterbury for supporting this research.

Notes and references

1 (*a*) P. J. Steel, *Acc. Chem. Res.*, 2005, **38**, 243–250; (*b*) T. R. Cook, Y.-R. Zheng and P. J. Stang, *Chem. Rev.*, 2013, **113**, 734–777; (*c*) L. Cronin, *Annu. Rep. Prog. Chem., Sect. A: Inorg. Chem.*, 2005, **101**, 348–374; (*d*) M. Albrecht, *Chem. Soc. Rev.*, 1998, **27**, 281–288.

2 (*a*) Y. E. Alexeev, B. I. Kharisov, T. C. H. Garcia and A. D. Garnovskii, *Coord. Chem. Rev.*, 2010, **254**, 794–831; (*b*) E. C. Constable, *Chem. Soc. Rev.*, 2013, **42**, 1637–1651.

3 (*a*) A. Frontera, P. Gamez, M. Mascal, T. J. Mooibroek and J. Reedijk, *Angew. Chem., Int. Ed.*, 2011, **50**, 9564–9583; (*b*) A. J. Lowe, B. M. Long and F. M. Pfeffer, *Chem. Commun.*, 2013, **49**, 3376–3388; (*c*) H. T. Chifotides and K. R. Dunbar, *Acc. Chem. Res.*, 2013, **46**, 894–906.

4 (*a*) M. M. Safont-Sempere, G. Fernandez and F. Wurthner, *Chem. Rev.*, 2011, **111**, 5784–5814; (*b*) B. Moulton and M. J. Zaworotko, *Chem. Rev.*, 2001, **101**, 1629–1658.

5 (*a*) J. G. Hardy, *Chem. Soc. Rev.*, 2013, **42**, 7881–7899; (*b*) M. Ruben, J. Rojo, F. J. Romero-Salguero, L. H. Uppadine and J.-M. Lehn, *Angew. Chem., Int. Ed.*, 2004, **43**, 3644–3662.

6 (*a*) S.-Q. Wu, Y.-T. Wang, A.-L. Cui and H.-Z. Kou, *Inorg. Chem.*, 2014, **53**, 2613–2618; (*b*) M. Walesa-Chorab, M. Kubicki, M. Korabik and V. Patroniak, *Dalton Trans.*, 2013, **42**, 9746–9754; (*c*) A. R. Stefankiewicz, J. Harrowfield, A. Madalan, K. Rissanen, A. N. Sobolev and J.-M. Lehn, *Dalton Trans.*, 2011, **40**, 12320–12332; (*d*) M. Ruben, E. Breuning, M. Barboiu, J.-P. Gisselbrecht and J.-M. Lehn, *Chem. – Eur. J.*, 2003, **9**, 291–299.

7 (*a*) B. L. Schottel, H. T. Chifotides, M. Shatruk, A. Chouai, L. M. Perez, J. Bacsa and K. R. Dunbar, *J. Am. Chem. Soc.*, 2006, **128**, 5895–5912; (*b*) P. N. W. Baxter, J.-M. Lehn, B. O. Kneisel and D. Fenske, *Angew. Chem., Int. Ed. Engl.*, 1997, **36**, 1978–1981.

8 (*a*) P. N. W. Baxter, J.-M. Lehn, G. Baum and D. Fenske, *Chem. – Eur. J.*, 2000, **6**, 4510–4517; (*b*) A.-M. Stadler, C. Burg, J. Ramirez and J.-M. Lehn, *Chem. Commun.*, 2013, **49**, 5733–5735; (*c*) A. Marquis, J.-P. Kintzinger, R. Graff, P. N. W. Baxter and J.-M. Lehn, *Angew. Chem., Int. Ed.*, 2002, **41**, 2760–2764.

9 (*a*) J. R. Price, N. G. White, A. Perez-Velasco, G. B. Jameson, C. A. Hunter and S. Brooker, *Inorg. Chem.*, 2008, **47**, 10729–10738; (*b*) J. R. Price, Y. Lan and S. Brooker, *Dalton Trans.*, 2007, 1807; (*c*) B. R. Manzano, F. A. Jalon, I. M. Ortiz, M. L. Soriano, F. Gomez de la Torre, J. Elguero, M. A. Maestro, K. Mereiter and T. D. W. Claridge, *Inorg. Chem.*, 2008, **47**, 413–428; (*d*) J. Kuzelka, S. Mukhopadhyay, B. Spingler and S. J. Lippard, *Inorg. Chem.*, 2004, **43**, 1751–1761.

10 (*a*) N. Parizel, J. Ramirez, C. Burg, S. Choua, M. Bernard, S. Gambarelli, V. Maurel, L. Brelot, J.-M. Lehn, P. Turek and

A.-M. Stadler, *Chem. Commun.*, 2011, **47**, 10951–10953; (*b*) M. Ruben, J.-M. Lehn and G. Vaughan, *Chem. Commun.*, 2003, 1338–1339; (*c*) A. R. Stefankiewicz, G. Rogez, J. Harrowfield, A. N. Sobolev, A. Madalan, J. Huuskonen, K. Rissanen and J.-M. Lehn, *Dalton Trans.*, 2012, **41**, 13848–13855; (*d*) J. Rojo, F. J. Romero-Salguero, J.-M. Lehn, G. Baum and D. Fenske, *Eur. J. Inorg. Chem.*, 1999, 1421–1428.

11 S. E. Bodman and C. M. Fitchett, *Dalton Trans.*, 2014, **43**(33), 12606.

12 (*a*) B. Gil, G. A. Cooke, D. Nolan, G. M. O'Maille, S. Varughese, L. Wang and S. M. Draper, *Dalton Trans.*, 2011, **40**, 8320–8327; (*b*) E. C. Constable, C. E. Housecroft, B. M. Kariuki, M. Neuburger and C. B. Smith, *Aust. J. Chem.*, 2003, **56**, 653–655.

13 F. Thebault, A. J. Blake, C. Wilson, N. R. Champness and M. Schroeder, *New J. Chem.*, 2006, **30**, 1498–1508.

14 H. Kon and T. Nagata, *Dalton Trans.*, 2013, **42**, 5697–5705.

15 (*a*) A. Atfah, A. H. Tuhl and T. S. Akasheh, *Polyhedron*, 1991, **10**, 1485–1490; (*b*) G. Cooke, G. M. O'Maille, R. Quesada, L. Wang, S. Varughese and S. M. Draper, *Dalton Trans.*, 2011, **40**, 8206–8212; (*c*) A. Golka, D. C. Craig and M. N. Paddon-Row, *Aust. J. Chem.*, 1994, **47**, 101–110.

16 (*a*) A. N. Khlobystov, A. J. Blake, N. R. Champness, D. A. Lemenovskii, A. G. Majouga, N. V. Zyk and M. Schroder, *Coord. Chem. Rev.*, 2001, **222**, 155–192; (*b*) J. Burgess and P. J. Steel, *Coord. Chem. Rev.*, 2011, **255**, 2094–2103; (*c*) P. J. Steel and C. M. Fitchett, *Coord. Chem. Rev.*, 2008, **252**, 990–1006.

17 E. C. Constable, C. E. Housecroft, M. Neuburger, S. Reymann and S. Schaffner, *Chem. Commun.*, 2004, 1056–1057.

18 (*a*) E. C. Constable, C. E. Housecroft, M. Neuburger, S. Reymann and S. Schaffner, *Eur. J. Inorg. Chem.*, 2008, 3540–3548; (*b*) E. C. Constable, C. E. Housecroft, M. Neuburger, S. Reymann and S. Schaffner, *Aust. J. Chem.*, 2008, **61**, 847–853.

19 N. Rahanyan, S. Duttwyler, A. Linden, K. K. Baldridge and J. S. Siegel, *Dalton Trans.*, 2014, **43**, 11027–11038.

20 (*a*) S. W. Kelemu, C. M. Fitchett, M. I. J. Polson, J. L. Wikaira and P. J. Steel, *J. Organomet. Chem.*, 2014, **749**, 129–133; (*b*) S. W. Kelemu and P. J. Steel, *CrystEngComm*, 2013, **15**, 9072–9079.

21 K. Chainok, S. M. Neville, C. M. Forsyth, W. J. Gee, K. S. Murray and S. R. Batten, *CrystEngComm*, 2012, **14**, 3717–3726.

22 R. Puttreddy and P. J. Steel, *CrystEngComm*, 2014, **16**, 556–560.

23 A. G. Young and L. R. Hanton, *Coord. Chem. Rev.*, 2008, **252**, 1346–1386.

24 C. M. Fitchett, C. Richardson and P. J. Steel, *Org. Biomol. Chem.*, 2005, **3**, 498–502.

25 (*a*) E. C. Constable, D. F. C. E. Housecroft and T. Kulke, *Chem. Commun.*, 1998, 2659–2660; (*b*) Y. Cui and C. He, *J. Am. Chem. Soc.*, 2003, **125**, 16202–16203.

26 (*a*) J. L. Gulbransen and C. M. Fitchett, *CrystEngComm*, 2012, **14**, 5394–5397; (*b*) C.-Q. Wan, Y. Zhang, X.-Z. Sun and H.-J. Yan, *CrystEngComm*, 2014, **16**, 2959–2968; (*c*) G. Dura, M. C. Carrion, F. A. Jalon, A. M. Rodriguez and B. R. Manzano, *Cryst. Growth Des.*, 2014, **14**, 3510–3529.

27 (*a*) D. Braga, S. d'Agostino, E. D'Amen and F. Grepioni, *Chem. Commun.*, 2011, **47**, 5154–5156; (*b*) E. Kim, H. Lee, T. H. Noh and O.-S. Jung, *Cryst. Growth Des.*, 2014, **14**, 1888–1894; (*c*) X.-C. Huang, D. Li and X.-M. Chen, *CrystEngComm*, 2006, **8**, 351–355; (*d*) M. Abul Haj, C. B. Aakeroey and J. Desper, *New J. Chem.*, 2013, **37**, 204–211.

28 (*a*) H. Xie, L. Zu, H. R. Oueis, H. L. J. Wang and W. Wang, *Org. Lett.*, 2008, **10**, 1923–1926; (*b*) N. Rahanyan, A. Linden, K. K. Baldridge and J. S. Siegel, *Org. Biomol. Chem.*, 2009, **7**, 2082–2092.

29 G. Sheldrick, *Acta Crystallogr., Sect. A: Found. Crystallogr.*, 2008, **64**, 112–122.

30 G. Sheldrick, *ShelXL-97*, Göttingen University, Göttingen, Germany, 1997.

31 O. V. Dolomanov, L. J. Bourhis, R. J. Gildea, J. A. Howard and H. Puschmann, *J. Appl. Crystallogr.*, 2009, **42**, 339–341.